Journal of Imaging Science and Technology® 50(2): 202–215, 2006.

Leveling During Toner Fusing: Effects on Surface Roughness and Gloss of Printed Paper

Torbjörn Pettersson▲ and Andrew Fogden
YKI, Institute for Surface Chemistry, Box 5607, SE-114 86 Stockholm, Sweden
E-mail: torbjorn.pettersson@surfchem.kth.se

Abstract. *The results of digital printing trials using a Xeikon press on uncoated and coated paper were analyzed using interferometric profilometry to characterize printed paper topography and toner film thickness. Solid print areas were fused at various temperatures, including radiant fusing with and without heated rolls. The overall surface roughness of the prints is slightly higher on the coated than uncoated paper, but is mainly dictated by transferred toner amount and fusing conditions. Increased toner coverage degree, or layer thickness, gives reduced surface roughness, provided the applied fusing power suffices. Increase in radiant fusing temperature yields a decrease in overall print roughness, however, this decrease is more pronounced on coated paper and higher toner amounts. Bandpass analysis of print surface roughness shows that short-scale roughness at or below the lateral length scales of toner particle dimensions always decreases with increasing radiant fusing temperature, whereas roughness contributions at wavelengths above* 10 μm *can increase, with this transition value being shorter on coated paper and at lower toner amounts. Print gloss after radiant fusing is strongly correlated to print roughness on wavelengths up to this transition length scale, and the correlation can extend to order* 100 μm *if complemented by heated roll fusing. © 2006 Society for Imaging Science and Technology.*
[DOI: 10.2352/J.ImagingSci.Technol.(2006)50:2(202)]

INTRODUCTION

The final step in electrophotographic printing processes is the permanent fixation of the applied toner image on the paper by the fusing subsystem.[1] In general, fusing involves the physical-chemical mechanisms of melting of the thermoplastic base polymer(s) of the toner, followed by particle sintering or coalescence, spreading on the paper surface and penetration into its pores, prior to resolidification.[2,3] Fusing can be performed with heated rolls, as in most modern office printers, in which the toner is bonded to the paper by the heat and pressure pulse applied in the nip between two rolls. Alternatively, fusing can be performed without applied pressure using infrared (IR) radiation, e.g., in digital web printing. Although the principal purpose of the fusing process is to create sufficient toner adhesion for subsequent processing and end use, the process also influences the optical print quality. In particular, fusing is essential in providing a high print gloss level. It also has a strong bearing on print density, as well as sharpness of edges, lines, and text quality. Thus the challenge is to provide a satisfactory compromise between these quality parameters with the given toner system, within the operational window of temperature, dwell time, and pressure of the fusing system, and for a sufficiently broad range of papers including uncoated and coated grades. To aid in satisfying these often conflicting requirements on process and product performance, a combination of radiant and heated roll fusing is provided on some digital presses. One example is the Xeikon press used in the current study, for which the hot nip is used as finishing roller after IR fixing.

As in all printing processes, a key quality issue for electrophotography is uniformity of the printed image. Unwanted local variations in gloss and optical density, and toner film coverage and thickness, over solid and half-tone printed areas can arise from a number of effects. The paper itself possesses lateral variations in topography (roughness), surface chemistry, and dielectric properties, over a spectrum of length scales. These factors, as well as other sources of variation in the toner transfer system, can lead to uncovered white specks in solid areas. Any failure of the fusing system to remove these white specks, or indeed any tendency for it to create them, can lead to serious losses and variations in optical density and gloss. Even in the case of speck-free solid areas, the surface roughness and thickness variations of the paper cause a locally varying contact pressure between fusing nip and paper, leading to peaks with high fusing degree and gloss (nip calendering) and valleys with lower fusing and gloss.[4,5] Owing to the relatively large dimensions of the toner particles (approximately 10 μm), electrophotography is also susceptible to the undesirable print features of differential gloss and three-dimensional surface relief.[6] In particular, in half-tone images a transition from low to high toner coverage can produce large variations in gloss, from paper-surface-controlled gloss below the midtones to fusing-controlled gloss above the midtones.[7] This collection of possible defects occur in both uncoated and coated papers, with the general perception that the consistently higher roughness of uncoated papers results in a lower, but robust, print quality, with coated papers exhibiting a higher quality but also a greater sensitivity.[4,5]

The above findings have been obtained using a range of different printer and toner systems, often with a separate tailor-made fusing unit in order to independently examine the effects of different fusing units and their various operational parameters. Aside from the normal quality measure-

▲IS&T Member

Received Sep. 2, 2004; accepted for publication Jun. 14, 2005.
1062-3701/2006/50(2)/202/14/$20.00.

ments of optical density and gloss, a number of standard and novel techniques have been applied to probe the fusing process and fused state. Toner adhesion and mechanical resistance properties are assessed using rubbing and scratching,[3] creasing and tape peeling, and IGT picking,[8] with the corresponding fusing quality measure found to depend on a combination of fusing pressure, dwell time, and local temperature (the latter enters via the toner's viscosity dependence). Microscopy or scanning, followed by image analysis, provides further information on defects within print areas and measures of the sharpness of print edges and lines, the spreading of points, and quality of text. A collection of spectroscopic techniques, including different Fourier-transform(IR) and Raman instruments, have been used to probe the toner layer structure, its chemistry and interactions with the paper substrate giving rise to its adhesion.[9]

Topography and surface roughness of the unprinted and printed papers can be quantified by a multitude of different instruments, giving direct or indirect height information over their particular measurement areas and subject to their particular limitations on resolution. Comparisons of these different methods are provided in Refs. 10 and 11. In the context of electrophotography, the relatively recently introduced technique of interferometric profilometry offers a number of advantages. Specifically, its lateral resolution is on the order of 1 μm, and with in principle no limit in vertical resolution, over image areas up to several millimeters in sidelength. This allows the noncontact imaging of all features from the finest scale of individual toner particles to macroscopic variations in paper (e.g., flocs) and print quality, and quantification of the surface roughness contributions from these various length scales by bandpass Fourier analysis. The surface roughness information can thus provide direct measures of toner sintering and spreading, the resulting local degree of fusing, the toner thickness, and three-dimensional print relief characteristics, and explain the origins of print gloss and its variations.

The current study applies this interferometric profilometry technique to analyze solid print areas produced by a Xeikon press with varying radiant and heated roll fusing conditions, on both uncoated and coated papers, and investigate the corresponding correlations to measured print gloss.

EXPERIMENT

Printing Trials

Rolls of two different papers for digital printing from Metsä Serla (now M-real) were used in the printing trials, namely one glossy coated paper (Galilei Art Gloss, 150 g/m^2) and one uncoated paper (Galilei Opal, 160 g/m^2). These papers had a caliper of 112 and 176 μm, respectively, with the coated paper having PPS value of 0.5 μm, while the uncoated paper had a Bendtsen roughness of 90 and 110 ml/min on the top (printing) and bottom sides, respectively. The topside of the printing form contained a photographic test image together with solid print (full tone) band fields (running in the cross direction) of 100% cyan (C), magenta (M), yellow (Y), and black (K), 200% blue (CM) and red (MY), 300% black (CMY), and 400% black ($CMYK$). The backside consisted of solid print band fields (running in the print direction) of no print, K, CM, CMY, and $CMYK$,with these fields occupying exactly the same area on the backside as the topside fields, providing a checkerboard matrix of topside-backside combinations.

Printing was performed using a Xeikon DCP 320 D press with the Xeikon toner system V2. These polyester based toner particles are produced by milling and have irregular morphologies, with a mean particle size of 8.8 μm. This Xeikon press has two types of fusing units, one radiant source (IR) followed by two pairs of heated rolls. The press was controlled so that the four process colors achieved their Xeikon standard print density values for normal printing and fusing conditions. These standard fusing conditions were 125 and 145 °C in the radiant unit and 100 and 110 °C in the heated rolls, for the coated and uncoated papers, respectively. The fusing was varied, without compensation in transferred toner amount, by using only the radiant source, only the heated nips, or the former followed by the latter. For the case of radiant fusing only, the temperature was varied in 5 °C steps over the ranges 105–145 °C and 120–150 °C for the coated and uncoated paper, respectively. For radiant fusing followed by the heated nips, the corresponding temperature intervals investigated were 120–130 °C (IR) and 95–105 °C (heated rolls), for coated paper, and 140–150 °C (IR) and 105–115 °C (heated rolls), for uncoated paper, i.e., as a 3×3 matrix of 5 °C increase or decrease from the standard fusing settings. In addition, unfused samples have been produced by pressing the emergency stop during press running and cutting out samples from the section of the paper web having not reached the fusing units.

Print Characterization

All topographical measurements of the printed and unprinted papers were performed using a white-light interferometric profilometer, NewView 5010, Zygo Corporation (USA).[12] The technique[13] is based on reflection of white light from the sample surface, which then interferes with the light reflected from an internal reference surface in the objective. Images over the sample are collected with a charge coupled device camera on scanning the objective in the height (z) direction. The resulting images are analyzed in the frequency domain giving a high-resolution three-dimensional image (height map) of the substrate topography. The vertical resolution is independent of the optics and is in principle unlimited, i.e., of the order of 0.1 nm over a range of 100 μm, whereas the lateral resolution depends on the objective used. All images in this study were taken with a $20\times$ lens, and zoom value of 2, giving an image rectangle of 175×130 μm with 0.88 μm lateral resolution and a maximum resolvable surface slope of 29.5°. Stitching together a 2×2 matrix of such adjoining rectangles, with 25% overlap, provided a larger rectangle of 311×233 μm, while maintaining the same resolution as the single rectangles. In all cases a least-squares fitted plane was removed from the original data in order to minimize the influence of macros-

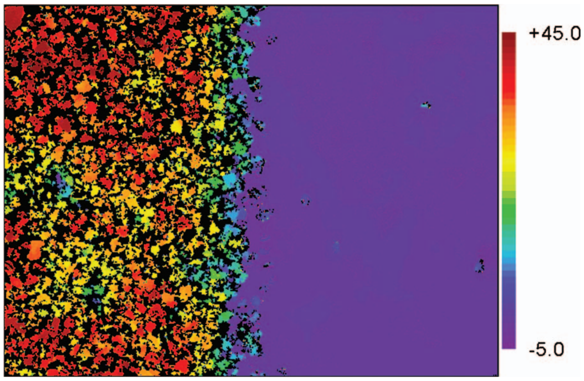

Figure 1. Topographical height map, of size 175×130 μm, at the edge between printed toner (unfused CMY, on the left hand side) and coated paper (right hand side). The color bar units are microns.

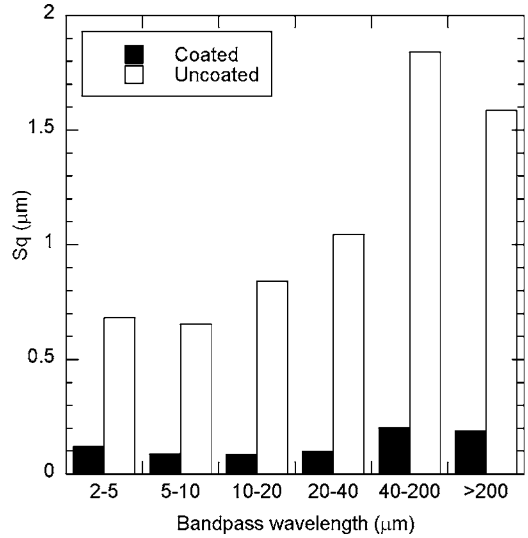

Figure 2. Surface roughness from interferometric profilometry on the coated and uncoated papers, divided into contributions from the different lateral wavelength bands.

cale orientational deviations due to sample tilt caused by errors in mounting or presence of backside print.

The raw images over these larger rectangles were fast Fourier transform filtered, either with a high (wavelength)-pass filter with a lower cutoff wavelength[14] of 5 μm or bandpass filtered keeping the bands 2–5, 5–10, 10–20, 20–40, 40–200, or >200, μm. From the high-pass and bandpass filtered images the root-mean-square (rms) surface roughness Sq was then calculated

$$Sq = \sqrt{\frac{1}{mn}\sum_{i=1}^{m}\sum_{j=1}^{n} z(i,j)^2}, \tag{1}$$

where m,n are the numbers of pixels in x,y, and $z(i,j)$ the local height of pixel (i,j) after removal of the least-squares fitted plane. All surface roughness values reported in this study are the mean of four different image areas, each of size 311×233 μm.

To evaluate the toner film thickness, topographical images of the smaller single rectangles were taken so as to include the edge of the printed area, i.e., transition from toner film to unprinted paper. One such image is shown in Fig. 1 for the boundary between the *CMY* print layer and the unprinted coated paper. A plane was least-squares fitted to the region of only paper and then subtracted from the entire image to give the toner film thickness from the resulting difference image. The thickness values reported here are the average of the height steps from five one-dimensional cross sections from one image area (175×130 μm).

In addition to the topographical characterization, gloss was measured on the printed and unprinted samples with a Zehntner ZGM 1020, Zehntner GmbH (Switzerland) at 75° angle using the Tappi standard[15] as guideline. Gloss was measured on the topside (mean value of three measurement points, and oriented in the cross direction) within areas for which no print was present on the backside.

RESULTS AND DISCUSSION

Unprinted and Unfused States

For the unprinted papers, the Sq (rms) surface roughness values from the Zygo profilometer using high-pass filtering above 5 μm are 0.383 and 3.329 μm for coated and uncoated paper, respectively, and the corresponding 75° gloss values are 72.6% and 9.0%. Figure 2 further shows the distribution of this surface roughness into the six wavelength bands discussed above. The roughness of the coated paper is obviously much lower across all bands. Normalization of these values to those for the maximum band (40–200 μm) reveals that the coated paper is proportionally rougher at the two shortest wavelengths, due to contributions from coating pigment microparticles, while the uncoated paper is proportionally higher over the next two bands (up to 40 μm), i.e., up to the length scale of the width of its individual fibers.

After transfer of the toner to these two paper substrates, the toner layer thickness and surface roughness were determined to provide the initial condition for the following analysis of the fused prints. The thickness of the unfused layers (as shown in Fig. 1) of the eight different colors on both the coated and uncoated papers are provided in Fig. 3. As expected, the values for the single color (100%) layers are approximately 15 μm, and twice, three times, and four times this thickness (i.e., 30, 45, and 60 μm) for the 200%, 300%, and 400%, layers, respectively. In particular, the mass density of the packing does not increase with the number of these layers. Note though that significant differences exist between the four single colors, with a hierarchy of increasing thickness from *Y* to *C* to *M* to *K*. Since all four toners have equal mean particle size, this hierarchy directly reflects the corresponding increase in degree of surface coverage of these particles, as verified from the topographical images. The substrate does not seem to affect significantly the unfused toner thickness.

Figure 4 plots the surface roughness of the unfused toner-transferred coated and uncoated papers as a function of the corresponding layer thicknesses in Fig. 3. This plot includes the surface roughness from high-pass filtration (all wavelengths above 5 μm) and two representative bandpass

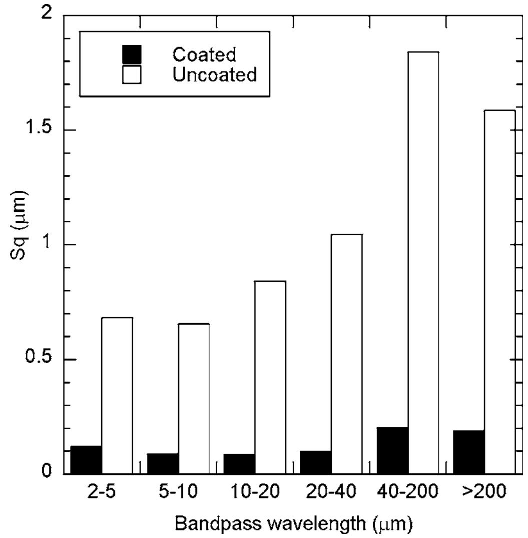

Figure 3. Mean layer thickness of unfused toner of the eight different color combinations on coated and uncoated paper, as determined by interferometric profilometry.

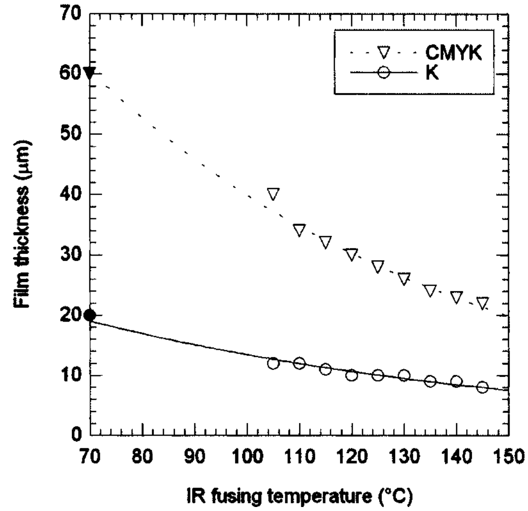

Figure 5. Toner layer thickness for 100% (*K*) and 400% (*CMYK*) black on coated paper, as function of radiant fusing temperature. The curves are exponential fits to the fused toner data points (open symbols), with their extrapolations to the toner softening temperature showing good agreement with the measured unfused layer heights (filled symbols).

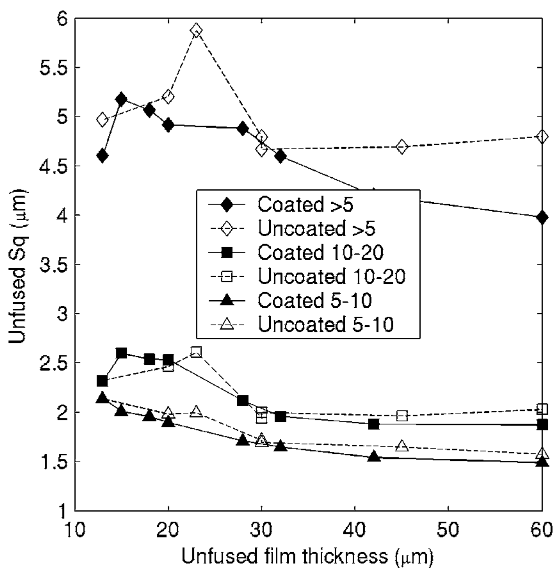

Figure 4. Surface roughness of toner-transferred coated and uncoated paper prior to fusing, also showing the contribution from the two wavelength bands 5–10 and 10–20 μm, as function of corresponding unfused toner layer thickness.

filtrations, 5–10 and 10–20 μm. For the two lowest wavelength bands, 2–5 (not shown here) and 5–10 μm, i.e., lateral length scales up to single toner particle dimensions, the roughness decreases with increasing toner layer thickness, owing to the associated reduction in number of isolated and exposed particles per unit substrate area. For the three higher wavelength bands, 10–20, 20–40, 40–200 μm (latter two not shown), the roughness increases with toner layer thickness up to a thickness of approximately 20 μm, i.e., equivalent to the highest 100% physical coverage, and then decreases at higher toner amounts. This reflects the increase in occurrence of particle clusters (pairs, groups of 3, 4, etc. particles) with increasing coverage amount up to the onset of formation of multilayers, leading to the roughness decrease due to filling-in and evening-out of these features. Since the high-pass filtered roughness removes the finest band, and is thus dominated by the longer wavelengths, its overall dependence on layer thickness in Fig. 4 follows roughly the form of these higher bands. Note that for all unfused samples the roughness values over all five bands are very similar on the coated and uncoated papers; the deviation between their total high-pass roughness curves in Fig.4 comes mainly from the highest wavelengths (above 200 μm) for which the uncoated paper variations give relatively poor statistical significance.

Fusing Effects on Print Thickness and Roughness

As mentioned above, the fusing of these toner particle layers was performed in three ways, namely with only the IR unit, or only the heated rolls, or the radiant heating followed by the hot nips. The first situation of only radiant fusing is the main focus of this study, with some attention also given later to radiant followed by hot roll fusing. Fusion using only the heated rolls gave runnability and print quality problems, since the partially melted toner stacked on the rollers and was thus transferred from its intended position to deposit on some other part of the sheet. This is due to the fact that the adhesion between the toner and rollers exceeded both the toner-paper adhesion and the cohesion within the toner film. The problem can be solved either by decreasing the toner-roller adhesion energy or increasing the toner film cohesion. The common way to implement the first solution is to change the surface energy of the rollers or add fusing oil, e.g., silicone oil, with low surface tension. In this study no such remedy was used, and these poor quality prints have not been evaluated.

The effect of the radiant fusing alone on the thickness of solid-print films is displayed in Fig. 5, showing the decrease for 100% and 400% black on coated paper over the IR tem-

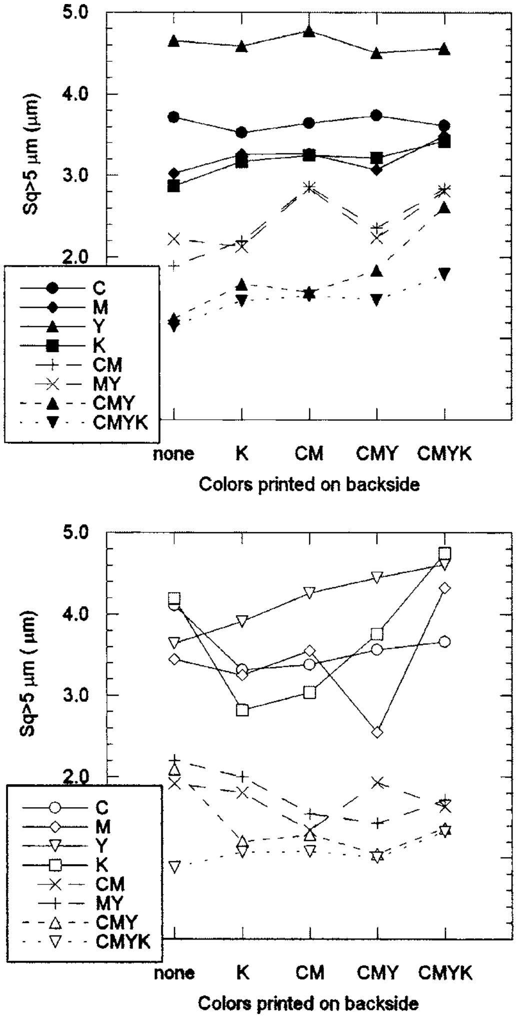

Figure 6. Total surface roughness, including all wavelengths above 5 μm, of topside solid prints (listed in legend) as function of the backside print (listed on horizontal axis), for both coated paper (above, filled symbols) and uncoated paper (below, open symbols). Fusing was performed with IR and heated roll at the standard conditions for each paper.

perature range 105–145 °C, and compared to the corresponding unfused thickness values in Fig. 3. As expected, the absolute decrease over this range is much more substantial for the thicker *CMYK* film (18 μm decrease) than for the *K* film (4 μm decrease). Note also that simple exponential curves shown in Fig. 5 not only give an accurate fit to the thickness evolution for both colors over this temperature range, but also on extrapolation to the toner softening temperature (70 °C) give very good agreement with the measured values for the unfused films.

We begin our in-depth analysis of the surface roughness of the printed toner films after fusing by mapping the general trends in color type, temperature, and influence of the backside print on the topside roughness. For this purpose it suffices to use to the overall *Sq* (rms) roughness measure containing all wavelength contributions above the 5 μm cutoff. The effect of backside print is shown in Fig. 6, for coated and uncoated paper, using IR followed by heated roll fusing at the standard temperature settings for each paper. In particular, the roughness of the eight topside colors is given as a function of the corresponding print on their backside (either 0%, 100%, 200%, 300%, or 400%). On the coated paper the topside roughness clearly decreases from 100% to 200% to 300% to 400% topside print, this being true independent of the type of print on the backside. Furthermore, the hierarchy in roughness of the 100% colors, with decreasing roughness from *Y* to *C* to *M* and *K*, precisely matches the trend of increasing unfused toner thickness in Fig. 3, indicating that this initial topside thickness (i.e., physical coverage) largely dictates its final roughness. Observe also that with increasing toner thickness up to 300% the increase in number of backside layers has a progressively stronger effect on increasing the topside roughness. This influence decreases again though on further increase to 400% topside print.

For the uncoated paper in Fig. 6 the level of topside surface roughness again decreases from 100% to 200% to 300% to 400% coverage, irrespective of backside coverage, however, the results show a higher degree of variation than on the coated paper. There is no clear hierarchy in topside roughness within the four 100% prints, nor any clear trends of increase or decrease as a function of backside print. Comparison of absolute values, for fixed topside and backside colors, reveals that the topside roughness is, more often than not, lower on the uncoated paper, although the opposite can be true for the case of no print on the backside. The tendency for lower print roughness on the uncoated paper, despite its significantly higher sheet roughness (Fig. 2), is partly due to its higher temperatures (145 compared to 125 °C for radiant, and 110 compared to 100 °C for heated nip) at these standard fusing conditions, and also to the slightly larger unfused film thicknesses (Fig. 3). The higher variability in the profilometry results for uncoated paper are, as mentioned above, a natural consequence of its less uniform structure on the length scales of the profilometric image sample rectangle, and thus requires sampling of a greater number of such areas to obtain truly reliable statistics.

Having analyzed the influence of the backside print, we refer all of the following results in this study to the printed topside areas with no print directly underneath them on the backside. Figure 7 focuses on the effect of the IR fusing temperature without any heated nip fusing, i.e., purely radiant, on both coated and uncoated paper. First, comparing these plots at the particular temperatures 125 and 145 °C matching the IR temperature for standard fusing conditions in Fig. 6, and taking the nonbackside-printed column in that figure, it can be seen that the extra fusing due to the heated rolls in Fig. 6 in general creates smoother surfaces, as anticipated. However, for the coated paper the nip increases roughness for Y, and for the uncoated papers the other 100% colors *C*, *M*, *K* have increased roughness. For the coated paper, these three colors *C*, *M*, and *K* give similar roughness in Fig. 7, with only a slight decrease with increasing IR temperature. The yellow gave the surprising result of increasing roughness with higher radiant fusing temperature (see below). The 200% colors give higher roughness at the low IR

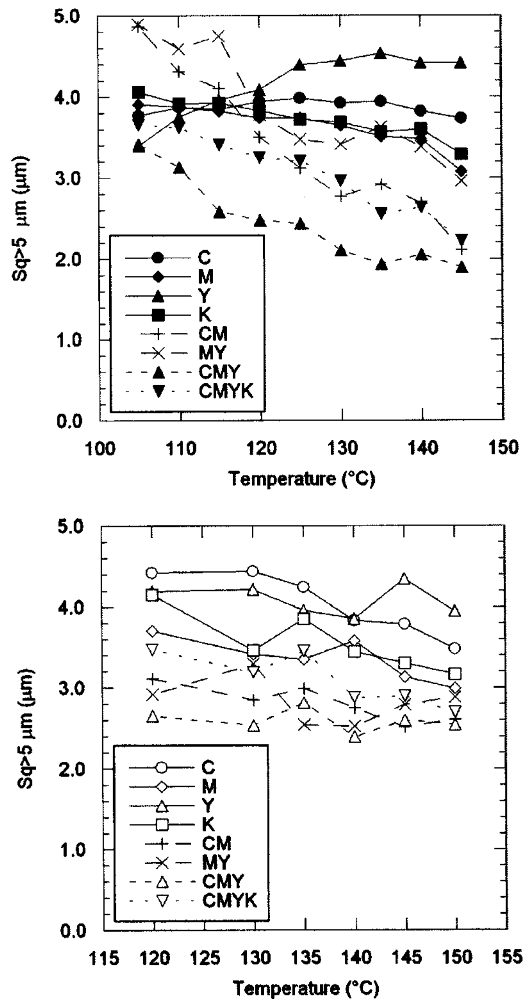

Figure 7. Total surface roughness of solid print areas of the eight different toner color combinations on coated paper (above, filled symbols) and uncoated paper (below, open symbols), as function of radiant fusing temperature, without heated roll fusing and with no backside print.

temperatures, but decrease steeply with increasing temperature to a roughness level intermediate to the 100% and 300%–400% levels. The most significant change in these trends from the standard fusing condition is that the 300% black is now smoother than its 400% counterpart, and so radiant fusing alone is apparently insufficient to further reduce surface roughness at the highest toner amount. For the uncoated paper in Fig. 7 the overall hierarchy in roughness is again from 100% (roughest) to 200% to 300% (smoothest), with 400% again giving high roughness breaking this trend. The main distinction from the coated paper in Fig. 7 is that the surface roughness of almost all layers now decreases only very slightly over this temperature range, especially so for the layers which already exhibit low roughness at the lowest IR temperature (120 °C).

Bandpass Analysis of Print Roughness

Further explanation of these interesting trends, both expected and unexpected, in the overall surface roughness during fusing requires subdivision of the topography into wavelength bands, as discussed above, in order to pinpoint the spatial origin of the effects. Figure 8 provides profilometry images of these different bandpass filtrations in order to illustrate the trends in corresponding surface roughness values discussed below. The example is for 100% black on coated paper, fused radiantly at the two extremes and midpoint of the temperature range examined, i.e., 105, 125, and 145 °C. The top row displays the unfiltered image, while the middle and bottom rows show the corresponding images for relatively low and high wavelength bands, 10–20 and 40–200 μm, respectively. The color range corresponds to the height scales shown (in microns), and the black textures (present on all images irrespective of wavelength) are regions in which the local slope is too steep (above 29.5°) for the profilometer to measure, typically occurring near the boundary between toner and paper. Observe from the unfiltered images that the toner particles have a strong tendency to build a network of linear chains of partly coalesced particles on the substrate (the blue background), which subsequently broadens, merges and flattens to give the texture at the highest fusing temperature. This behavior is analogous to that observed by Sipi et al.[4,5] using optical microscopy, namely that the uncovered white specks are small, evenly distributed and have sharp edges at low IR fusing temperatures, and become fewer, but larger and with softer edges at higher temperatures. From the shorter-wavelength band (middle column in Fig. 8) it is apparent that the finer features on the single-particle level progressively disappear on increasing fusing temperature, as would be expected from this coalescence and merging. On the other hand, the larger-wavelength band images (lowest column) show that this transformation of fine to course structures on merging actually leads to an increased roughness on these length scales, even though the overall height variations diminish. These trends, applying to all toner colors, will be quantified in the surface roughness analysis below.

Figure 9 displays the *Sq* (rms) surface roughness corresponding to each of the five wavelength bands for all eight toner layer types on coated paper. The highest band (wavelengths above 200 μm) is omitted, since these length scales approach those of the image area size, and therefore have lower statistical significance. Note that the overall levels of surface roughness for these five bands are of the same order of magnitude, but with significant differences in behavior as functions of temperature and toner layer type. For the two lowest wavelength bands, from the lateral resolution limit to 10 μm, the roughness decreases monotonically with temperature for all colors (as shown in Fig. 9), due both to smoothening of individual toner particle profiles and their merging with a neighbor to eradicate the gap in-between. Yellow gives clearly the highest roughness values in these two bands, mainly reflecting the fact that its layer contains the highest area density of isolated particles due to its lowest physical coverage, and thus that comparatively high temperatures are required for sufficient particle spreading to occur to enable merging. Further, a small fraction of finer particles is also left exposed in the spaces between the larger particles. With increasing toner physical coverage, from *Y* to

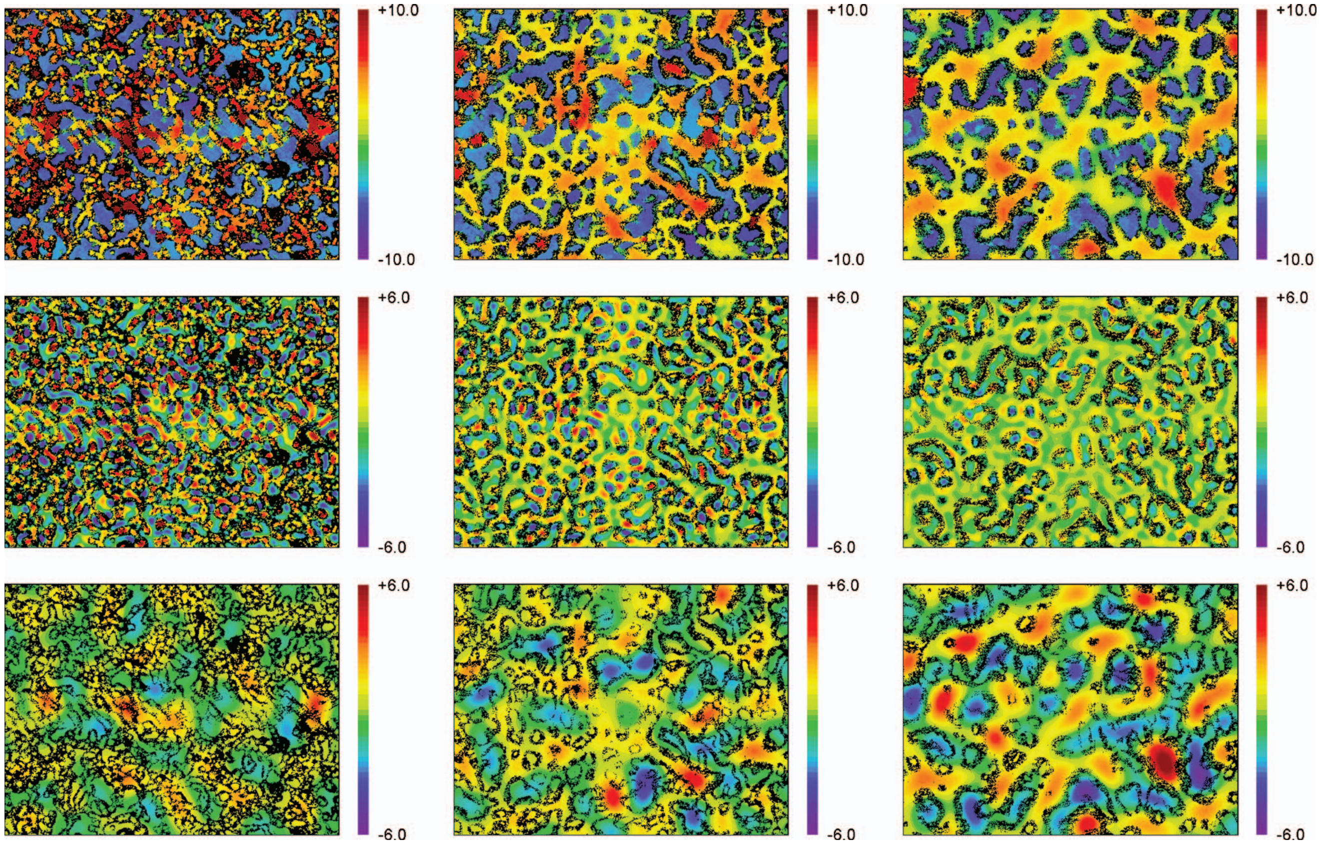

Figure 8. Representative topographical height maps over areas 311 × 233 μm, for 100% black on coated paper, fused radiantly at the three temperatures 105 °C (left column), 125 °C (middle), and 145 °C (right). The upper row shows the unfiltered images, whereas the middle and lower rows correspond to their bandpass filtrations in the wavelength intervals 10–20 and 40–200 μm. The color bar height units are microns.

C to *M* and *K*, this short-scale roughness progressively decreases, corresponding to fewer jumps due to isolated particles. All of the other toner layers (from 200% to 400%) fall on roughly a similar level to these three 100% colors, since once a reasonably complete layer is established, addition of further layers has little effect, as the slight reduction in interparticle spacing is counterbalanced by increase in number of particles contributing per unit image area.

At the next wavelength band of 10–20 μm (up to around twice the average particle diameter) in Fig. 9 the roughness again decreases with temperature for all colors, now excepting yellow, corresponding to the continued general merging of particles, pairs, and small clusters to remove their interparticle gaps. This decrease is most steep for the 100% and 200% layers, and less so for the thicker (300% and 400% black) layers for which their reduced interparticle separation and multiple contacting layers affects the merging transition already at shorter length scales and lower temperatures. The 100% black displays the highest roughness and strongest decrease owing to it starting with the highest density of unconnected particle pairs and small clusters. The yellow displays completely the opposite trend of increasing roughness in the 10–20 μm band, since isolated single particles spread during heating to increase diameter, but still often not fully merging, forcing the individual particle roughness contribution into this higher wavelength band. At the next higher band, 20–40 μm, the roughness of 100% *C*, *M*, and *K* first increases with temperature, then decreases, reflecting the continued particle and cluster merging which creates features at this length scale and which then merge further at the higher temperatures and begin contributing to the even higher band. The 400% layer (which always lies below the 300%) displays a slight decrease since the losses due to multiply merged particles on this length scale merging further exceed the gains of single particles (of which few are present) merging to enter this band. Yellow continues to increase for the opposite reason. At the highest band of 40–200 μm all colors increase their roughness with temperature (e.g., see Fig. 8) due to contributions from merging at the smaller length scales, which more than outweighs the general tendency to flattening (with no nip pressure applied).

Figure 10 displays the corresponding bandpass analysis of surface roughness of the toner layers fused radiantly on uncoated paper. Comparison of the overall levels with those in Fig. 9 reveals that the IR-fused printed paper roughness is similar in magnitude for uncoated and coated, despite the substantially lower roughness of the coated paper in Fig. 2. This clearly reflects the fact that the toner rather than the substrate provides the dominant contribution to printed pa-

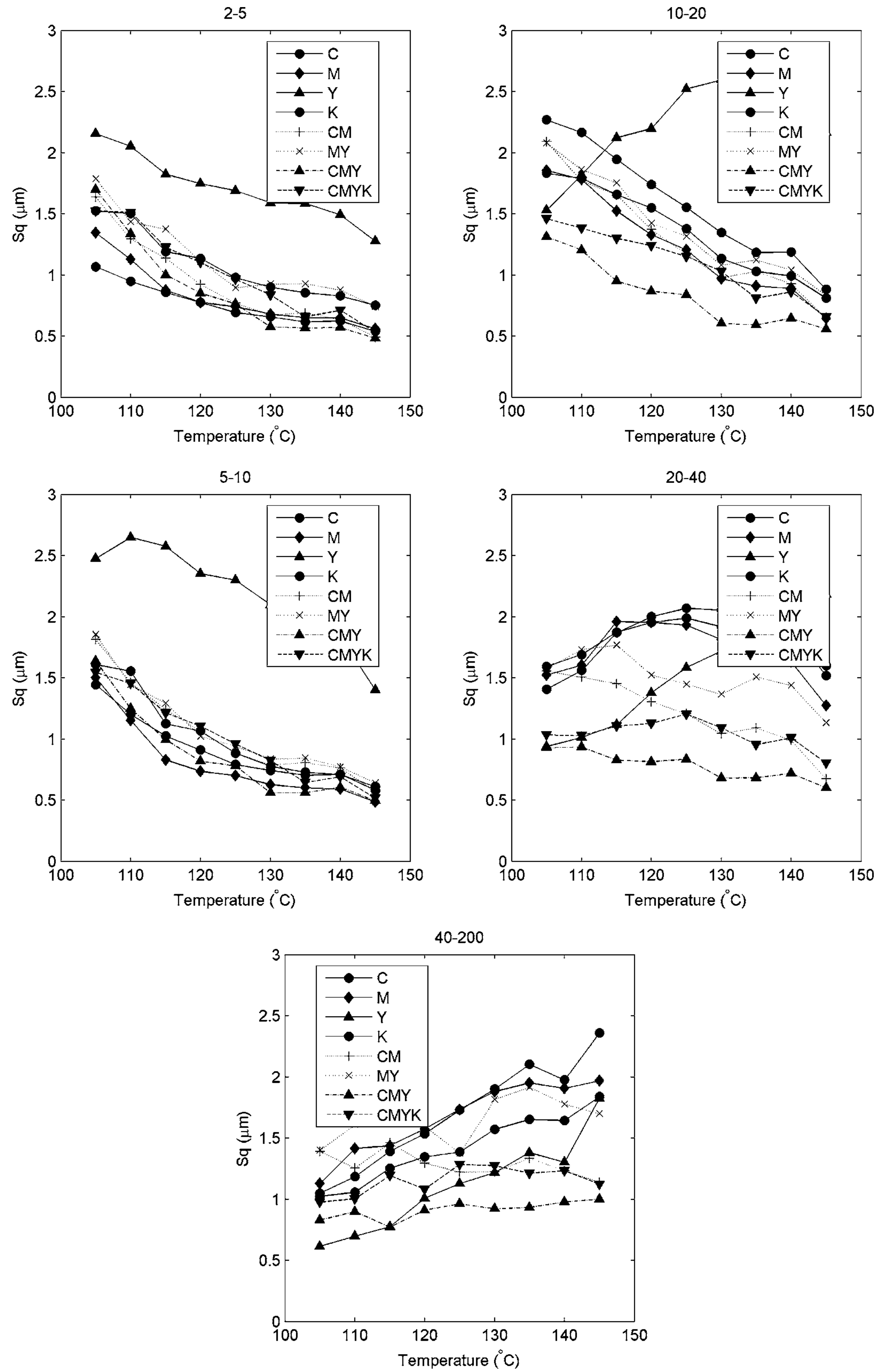

Figure 9. Surface roughness of toner films of the eight color combinations on coated paper, divided into the five wavelength bands indicated in microns, in each case plotted as a function of radiant fusing temperature (without heat rolls).

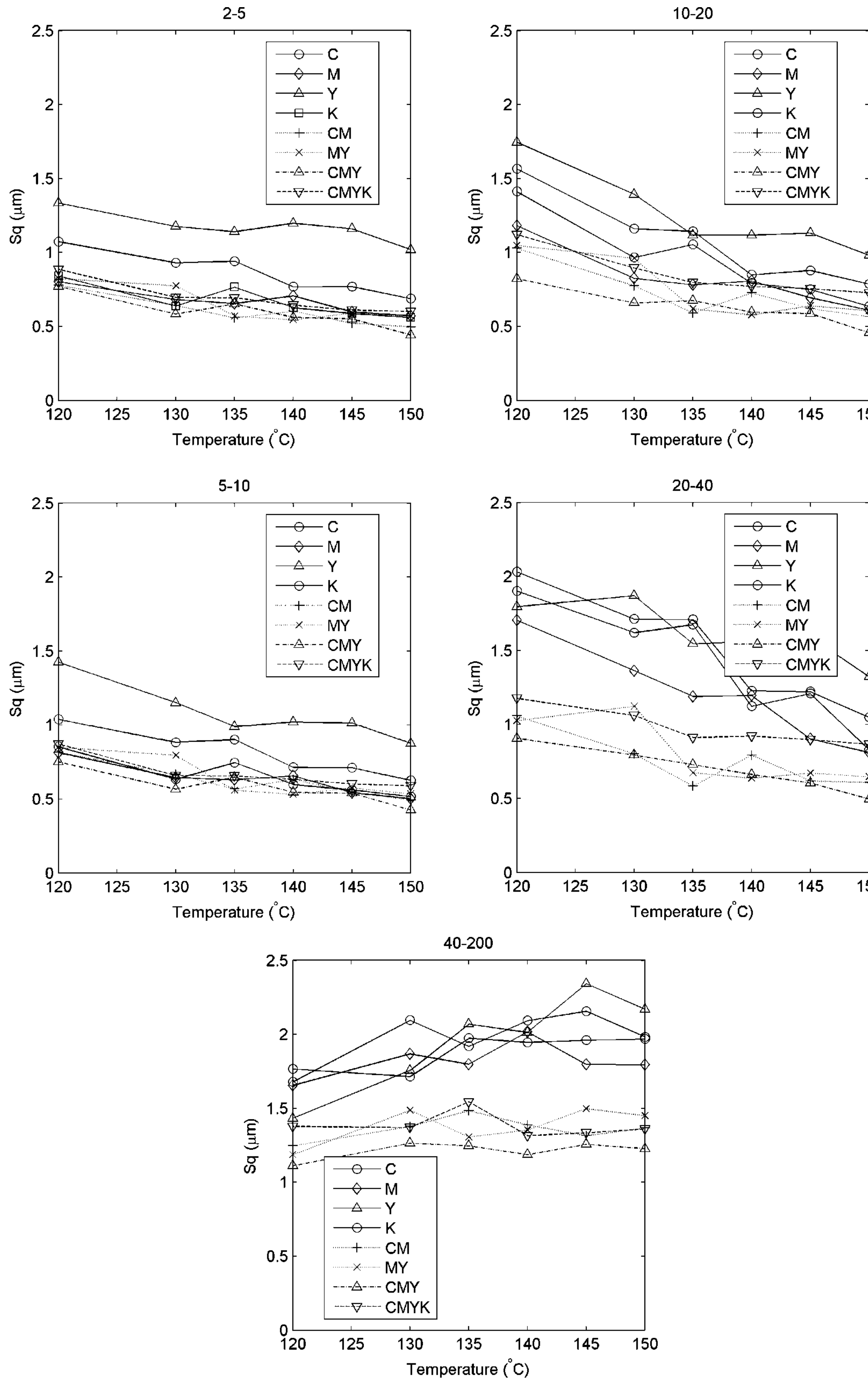

Figure 10. Surface roughness of toner films of the eight color combinations on uncoated paper, divided into the five wavelength bands indicated in microns, in each case plotted as a function of radiant fusing temperature (without heat rolls).

per roughness. Indeed, as also seen in Fig. 6, the uncoated paper tends to give somewhat lower print roughness than the coated, whether compared at the same temperature, or the different midpoints of their respective temperature ranges, with the exception of the 40–200 μm band that most strongly contributes to sheet roughness. This implies that the toner is better able to merge and flatten on the uncoated paper, principally due to its ability to sink into the interfiber void space rather than remaining exposed on the flat and relatively impervious coated paper. This is supported by the fact that, whereas the coated paper roughness at all length scales always increases significantly on printing, for uncoated paper the roughness at each band is relatively similar before and after printing, having a tendency to begin slightly higher (at the lowest IR fusing temperature) and end slightly lower (at the highest temperature), or vice versa at the longest wavelength band.

In common with the coated paper trends, the surface roughness of the printed uncoated paper decreases with temperature throughout the first three bands in Fig. 10 (now with yellow following this same trend), but now continues to decrease monotonically in the fourth band, and again increases with temperature in the longest band. Over the three short wavelength bands up to around 20 μm the roughness of the four 100% colors on uncoated paper decreases in order of increasing unfused film thickness, i.e., from *Y* to *C* to *M* and *K*, with the multiple colors (200%–400%) all lying grouped at roughly the level of the thicker 100% colors. For the 20–40 μm band a crossover occurs, with the four 100% colors behaving more similarly to each other and all having higher roughness than the multiple layers, a trend that continues through the longest wavelength band. The absence of the fusing-induced roughness increase for wavelengths 10–40 μm observed for some of the 100% colors (most notably yellow) on coated paper is again due to the sinking-in effect for uncoated paper. Thus although the number of objects contributing to these multiple-particle length scales increases due to particle spreading and merging with neighbors, the amplitude decrease more than compensates for this. It is only at the longest wavelengths that the increased contribution from merging outweighs their flattening. The 100% colors all behave similarly at these longer wavelengths (relative to 200% layers and more) since they do not give a sufficiently thick film to be able to blanket-out the fiber and fiber-fiber crossing features of the uncoated papers.

The correlation between these band contributions to printed paper surface roughness and the toner film height, for the cases of 100% and 400% black on coated paper (see Fig. 5), are plotted in Fig. 11. In this case the fusing is again only radiant, with each pair of points corresponding to temperature increasing in 5 °C steps from 105 to 145 °C (from right to left). The temperature-induced decrease in surface roughness in all of these shorter-wavelength bands is naturally associated with the decrease in film thickness. Note that the surface roughness decrease for a given thickness decrease becomes more dramatic with increasing roughness wavelength band for 100% black, mainly owing to the higher

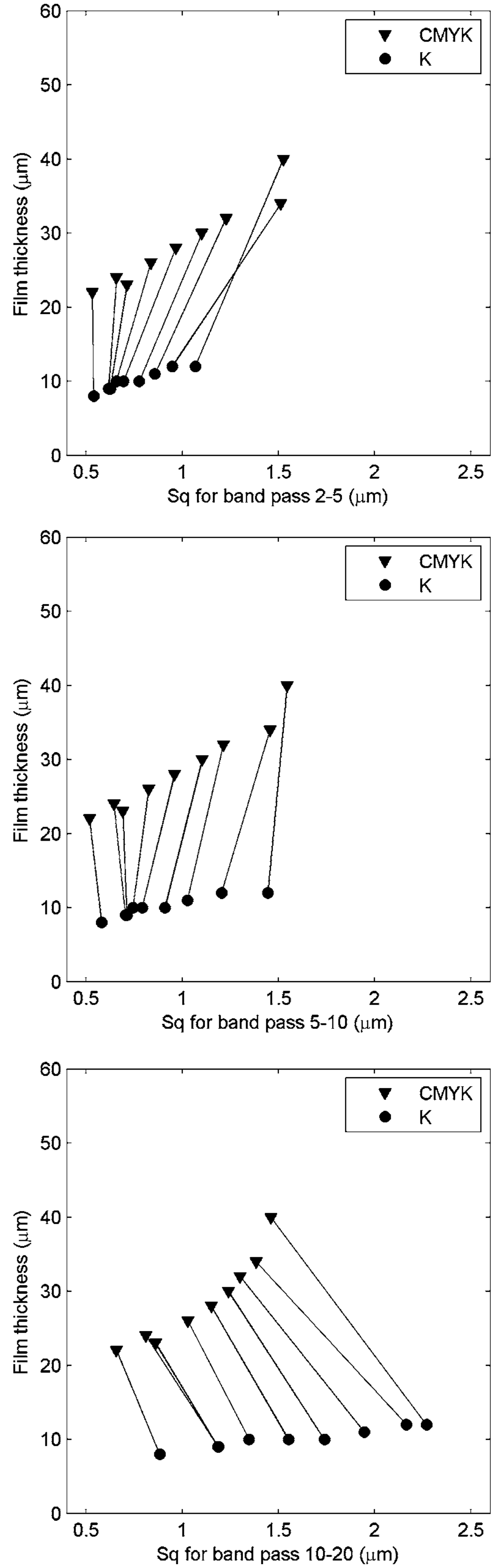

Figure 11. Measured toner film height for 100% (*K*) and 400% (*CMYK*) black printed on coated paper, as function of the corresponding surface roughness divided into the three lowest wavelength bands. In each case the nine points correspond to the nine increasing fusing temperatures (radiant without nip) from 105 °C (highest roughness) to 145 °C (lowest), with lines connecting the common temperatures.

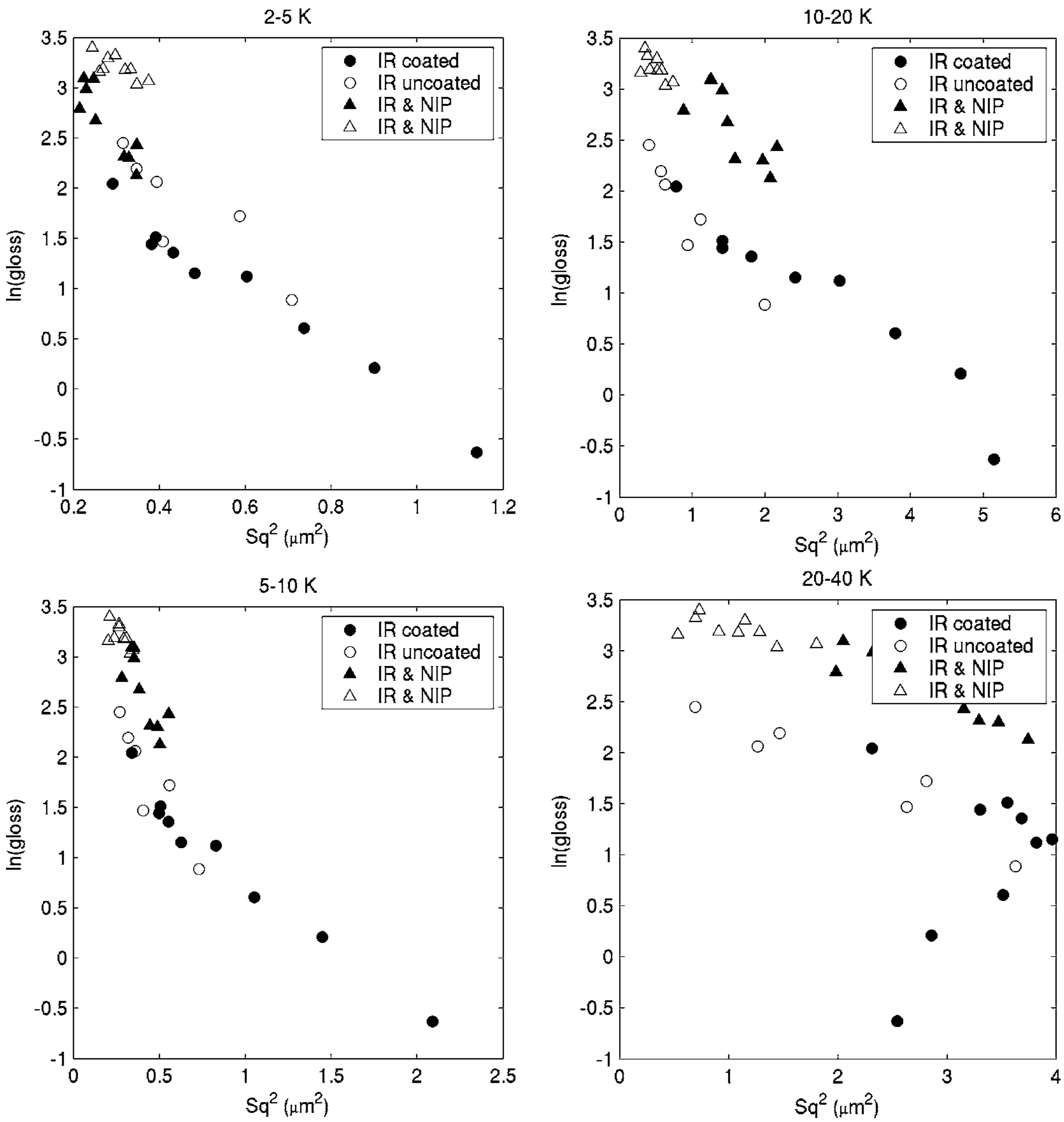

Figure 12. Logarithm of measured print gloss of 100% black toner films plotted as function of the square of their surface roughness separated into the four wavelength bands indicated (in microns). Each graph includes results on both coated (filled symbols) and uncoated (open), and both IR fusing alone (at the nine and six temperatures in Figs. 9 and 10, respectively) and followed by heated nip (at the nine temperature combinations given in the Experimental section).

unfused roughness amplitudes at these increased wavelengths. The 400% black behaves oppositely, with roughness decreasing more gradually with decreasing film height as the roughness wavelength increases. This illustrates the fact that in the radiant fusing of single layer films the particle merging greatly reduces roughness at this particle scale, with comparatively slight decrease in thickness, whereas for multilayer films the decrease in film porosity and, hence, thickness occurs with less effect on decreasing top layer roughness at these length scales. The height increase from 100% to 400% is thus associated with an increasing surface roughness at the shortest lateral length scales (since individual toner particle roughness exceeds that of the coated paper) but a decreasing roughness at longer scales (due to the increased scope for particle merging and removal of single particle boundaries).

Correlations Between Print Roughness and Gloss

Given this analysis of printed paper surface roughness, the question then arises as to what degree these various bands contribute to the measured print gloss. The standard formula[16,17] predicts that the gloss depends inversely on the exponential of the square of the rms surface roughness, i.e., that gloss on a logarithmic scale falls linearly with this mean square roughness

$$\frac{I}{I_0} = f(n,\theta)\exp\left[-\left(\frac{4\pi\sigma\cos\theta}{\lambda}\right)^2\right]. \qquad (2)$$

Here I_0 and I denote the intensities of the incident and reflected light, θ is their angle, and λ is the wavelength, σ is the surface roughness, and $f(n,\theta)$ the Fresnel coefficient of specular reflection as a function also of substrate refractive

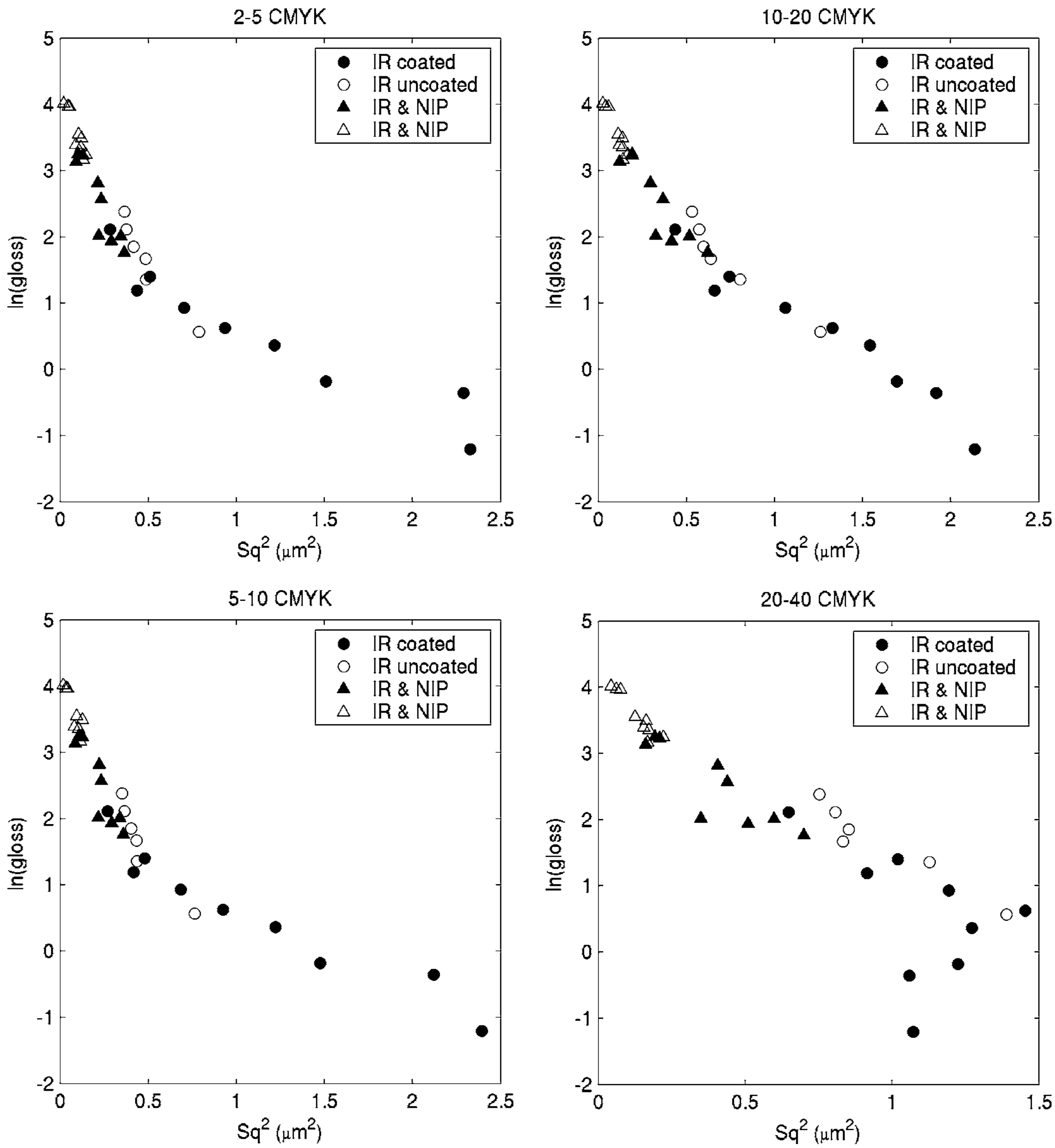

Figure 13. Logarithm of measured print gloss of 400% black (*CMYK*) toner films plotted as function of the square of their surface roughness separated into the four wavelength bands indicated (in microns). Each graph includes results on both coated (filled symbols) and uncoated (open), and both IR fusing alone (at the nine and six temperatures in Figs. 9 and 10, respectively) and followed by heated nip (at the nine temperature combinations given in the Experimental section).

index, n. The Tappi standard uses an angle of 75°, and white light with average wavelength 550 nm, and normalizes Eq. (2) to 100% for a black opaque optically smooth reference surface with corresponding refractive index of 1.540. Since gloss originates from microscale topography, the very short scale contributions are the most relevant choice for roughness σ in this context. Extra factors have been proposed to account for longer scale roughness modulations of this inherent gloss level and other effects.[18] Correlations between gloss (and gloss variations) and visual perception of paper and print quality have been investigated in a number of studies.[19]

To test the theory in Eq. (2), the correlation between the surface roughness band decomposition for the four first bands in Figs. 9 and 10 for coated and uncoated paper and the measured print gloss are plotted in Figs. 12 and 13 for 100% and 400% black, respectively. Here the results for the purely IR fusing, over the temperature ranges shown in Figs. 9 and 10, are combined with those from IR and heated roll fusing, with the matrixes of temperatures for coated and uncoated papers listed in the Experimental section.

In general for all colors, not just the two blacks shown in Figs. 12 and 13, the relation between gloss on a logarithmic scale and square of Sq for each of the four substrate-fusing type combinations is approximately linear with negative slope, as expected from the simple theory, provided the roughness from the three shortest wavelength bands is used. This is especially clear for the print types fused with only radiant heat, over which a wide range of roughness and gloss values are obtained at the different temperatures. In this case

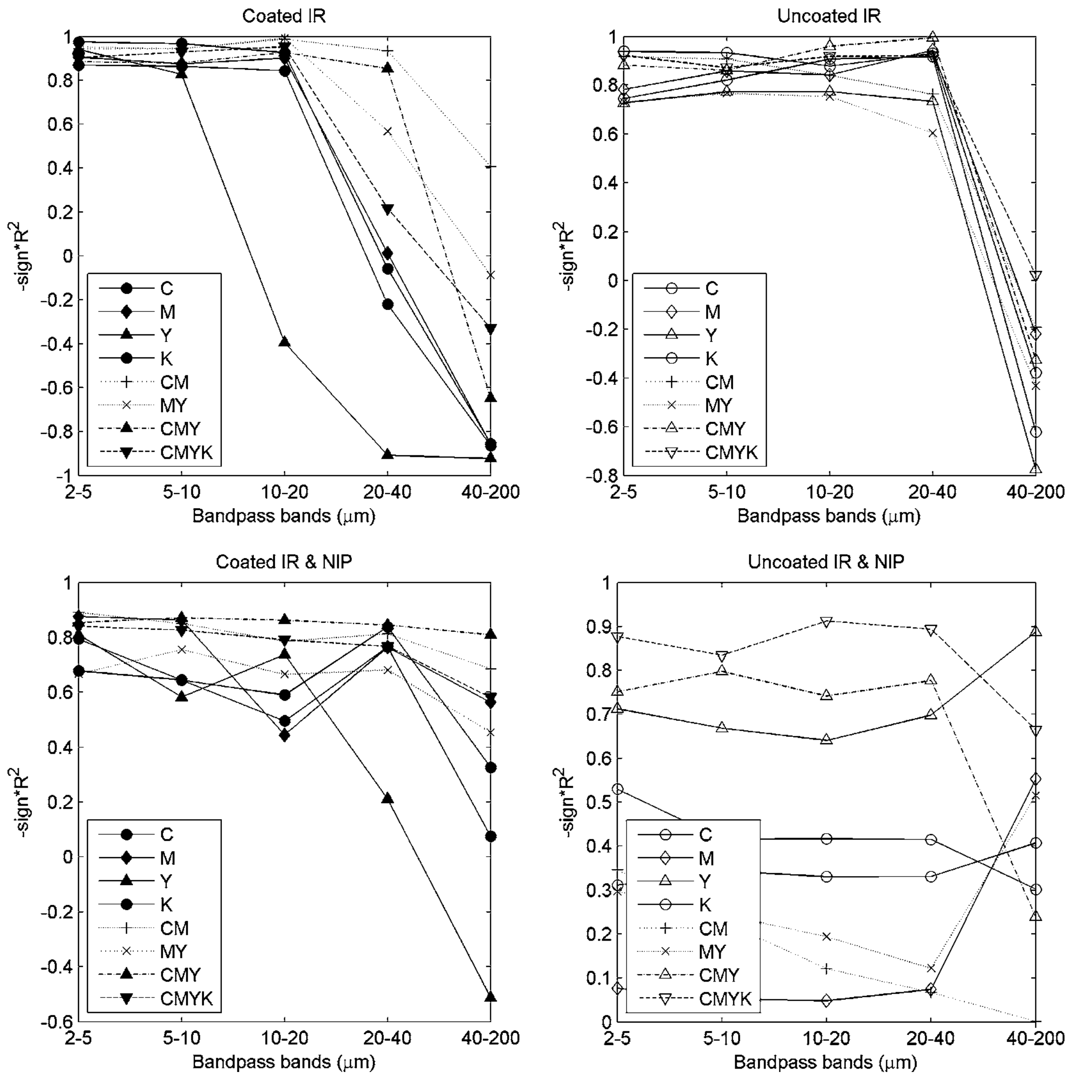

Figure 14. Coefficient of determination, R^2, of the least-squares fits of the gloss-roughness plots in Figs. 12 and 13 to straight lines, for all eight color combinations, on coated paper (upper two images) and uncoated paper (lower), and with IR fusing without heated nip fusing (left two images) and with heated nip (right). The coefficient varies from +1, indicating perfect fit to a negative sloping line, to −1, indicating perfect fit to a positive sloping line.

the magnitude of the slope is generally greater for the uncoated paper prints, meaning that the same reduction in surface roughness (squared) gives a greater reward in gloss. This can be a result of the fact that some of the surface roughness due to toner particles in crevices between fibers in the uncoated paper is detected by the profilometer but not by the 75° light in the gloss measurement. For the curing with IR followed by heated roll the trends are slightly less clear, owing to the narrow range of very low roughness and very high gloss values obtained, in turn due to the high radiant temperatures used plus the added effect of the rolls.[4,5] However, it appears that the slopes in these cases are also high, at roughly the level of those for purely IR fusing on uncoated paper, for all colors (excluding the exceptional behavior for yellow). The extra glossing benefit of the heated rolls is obviously the direct result of toner particle flattening, on the microscale, as well as increasing orientation over more macroscales to increase the number of areas contributing to the same 75° reflection.

For the fourth wavelength band (20–40 μm), the correlation between gloss and surface roughness persists for all colors (excepting yellow) and for all substrate-fusing types excluding purely IR fusing on coated paper. The latter gives poor correlation for the colors in Fig. 9 for which this band does not give decreasing roughness with increasing IR temperature. In particular, the low fusing temperatures give low roughness values since the particles have not merged sufficiently to give sizes contributing to this band, however, the gloss is still very low, as apparent from the particles' contribution to lower wavelength roughness. For this same reason the roughness-gloss theory gives poor agreement for the yellow toner, owing to its low physical coverage. Indeed for the wavelengths 10–40 μm the yellow prints on coated paper give an artificial correlation between increasing roughness and increasing gloss, simply reflecting the fact that the increasing roughness is the result of particle merging, thus decreasing the shorter wavelength roughness that truly correlates with the increased gloss. Note also that due to this low coverage for yellow, the gloss-roughness relations for the different fusing types give very different results, since melting-induced merging is limited and only the nip pressure is capable of flattening the isolated particles, resulting in much higher gloss.

Figure 14 summarizes the correlation between the printed paper gloss and surface roughness in these five bands, i.e., the R^2 coefficient of determination of best fit of a straight line to logarithm of gloss versus squared *Sq* roughness. In distinction to the usual R^2 definition, the values used here are signed according to the sign of the slope, so that negative slopes, in agreement with Eq. (2), give positive values (i.e., approaching $R^2 = +1$ with better linear fit). On the other hand, spurious effects such as the correlation of increasing roughness with gloss for yellow on coated paper mentioned above give negative R^2 values. For purely radiant fusing on coated paper the print gloss of all colors except yellow is strongly correlated to roughness in the lateral scale up to 20 μm, and ceases to be related at longer wavelengths, especially for the 100% colors. On uncoated paper the correlation is somewhat weaker for most colors (mainly as a side effect of their limited range of roughness and gloss values and thus greater sensitivity to measurement errors), but holds up to longer roughness length scales of around 40 μm. For radiant fusing followed by the heated rolls the correlations are even weaker due to the tight clustering of high roughness and gloss values, especially so for the uncoated paper prints. While this limits the interpretability of the results, it appears at least for coated paper that the correlation between roughness and gloss can extend to the largest length scales (up to 200 μm), especially for the thick toner films. This is clearly an effect of the increased degree of long-range orientation of local topography due to the flattening action of the nip.

CONCLUSION

This study has illustrated the utility of the white-light interferometric profilometer in quantifying the thickness and surface roughness spectral decomposition of toner layers transferred and fused on paper substrates, thus giving increased insight into the mechanisms giving rise to toner print quality. As expected, significant differences in surface roughness behavior were observed between the eight different toner color combinations, as a function of both substrate type (coated and uncoated paper) and fusing units (radiant and heated roll) and their temperature settings. Although the transferred toner amount is clearly the most important input parameter, it is possible that the toner chemistries of the four process color particles also contribute to these observed differences. For this reason it would be of interest to study, with this same profilometric technique, the fusing behavior of these four colors, not at their standard optical densities (as performed here) or even equal optical density, but rather at constant physical coverage, i.e., transferred particles per substrate area. While this is not a relevant comparison for optical properties, it would facilitate an evaluation of the differences between the physical-chemical spreading and merging abilities of the four toner types, and thus also provide insight into the adhesional properties of the particles and films. Furthermore, the study should be extended to other digital printing presses to check whether the same mechanisms are in action and, if so, develop a quantitative model of the phenomena.

ACKNOWLEDGMENTS

This research project was carried out within the Swedish national framework of the Surface Science Printing Program S2P2. The authors thank Framkom for providing access to their Xeikon press, and in particular Lars Forsberg for assistance in the planning and execution of the printing trials.

REFERENCES

1. D. M. Pai and B. E. Springett, "Physics of electrophotography", Rev. Mod. Phys. **65**(1), 163 (1993).
2. L. H. Lee, "Thermal fixing of electrophotographic images", in *Adhesion Science and Technology*, edited by L. H. Lee (Plenium, New York, 1975), Vol. 9B, pp. 831–852.
3. R. B. Prime, "Relationship between toner properties, fuser parameters, and fixing of electrophotographic images", Photograph. Sci. Eng. **27**(1), 19 (1983).
4. K. M. Sipi, M. Lamberg, and P. T. Oittinen, "Print quality in contact and non-contact fixing", *Proc IS&T's NIP15* (IS&T, Springfield, VA, 1999) pp. 426–429.
5. K. M. Sipi and P. T. Oittinen, "Print quality with hot roller and IR-radiation fixing methods", J. Imaging Sci. Technol. **44**(5), 442 (2000).
6. C. J. Wang, "Differential gloss in electrophotography", *Proc. IS&T's NIP15* (IS&T, Springfield, VA, 1999) pp. 406–407.
7. J. C. Briggs, M.-K. Tse, D. A. Telep, and J. Cavanaugh, "The effect of fusing on gloss in electrophotography", *Proc. IS&T's NIP14* (IS&T, Springfield, VA, 1998) pp. 456–461.
8. L. Leroy, V. Morin, and A. Gandhi, "Electrophotography: Effects of printer parameters on fusing quality", *Proc. 11th Intl. Printing and Graphics Arts Conf.* (IPGAC, Bordeaux, France, 2002).
9. K. M. Sipi, "Toner layer structure and toner adhesion on coated paper", *Proc. IS&T's NIP17* (IS&T, Springfield, VA, 2001) pp. 145–150.
10. N. F. Santos, A. Kholkin, and J. Velho, "Coating paper surfaces analysis using afm, sem and raman spectroscopy", *Proc. 11th Intl. Printing and Graphic Arts Conf.* (IPGAC, Bordeaux, France, 2002) pp. X–1.
11. P. Wagberg and P. A. Johansson, "Surface profilometry—a comparison between optical and mechanical sensing on printing papers", Tappi J. **76**(12), 115 (1993).
12. *New View 5000 Operating Manual OMP-0423D* (Zygo Corp., Middlefield, NJ, 1999).
13. P. De Groot and L. Deck, "Surface profiling by analysis of white-light interferograms in the spatial-frequency domain", J. Mod. Opt. **42**(2), 389 (1995).
14. K. J. Stout, *Development of Methods for the Characterisation of Roughness in Three Dimensions* (Penton, London, 2000).
15. T. Mitsuya and T. Kumasaka, "Heat-transfer and toner melting in an electrophotographic fuser system", J. Imaging Sci. Technol. **36**(1), 88 (1992).
16. T. K. Chinmayanandam, "On the specular reflection from rough surfaces", Phys. Rev. **13**(2), 96, (1919).
17. D. I. Lee, "A fundamental study on coating gloss", *Proc. TAPPI Coating Conf.* (TAPPI Press, Atlanta, GA, 1974) pp. 97–114.
18. P. Oittinen, "Surface reflection of coated papers and prints", in *Adv. in Printing Sci. Technol.*, Vol. 15, edited by W. H. Banks (Pentech, London, 1979), pp. 344–372.
19. M. A. Macgregor, P. A. Johansson, and M.-C. Béland, "Measurment of small-scale gloss variation in printed paper", *Proc. 1994 Intl. Printing and Graphic Arts Conf.* (IPGAC, TAPPI Press, Atlanta, GA, 1994) pp. 33–43.